DOI: XXXXXXXXXXXXXXXXXXXX - ISSN: XXXX-XXXX - Vol 1(1), 2025, pp: XX:XX

MECHANICS
OF SMART STRUCTURES
Available Online at: http://jmss.qut.ac.ir/

QOM UNIVERSITY OF TECHNOLOGY

Torsion of single-walled carbon nanotubes using new nanomechanical model with considering the chiral effects

ARTICLE INFO

Authors

Mohammad Reza Ebrahimian[1]

[1] Department of Mechanical Engineering, Kar Higher Education Institute, Qazvin, Iran, ebrahimian.reza@gmail.com

*** *Correspondence***
Address: Department of mechanical Engineering Kar Higher Education Institute, Qazvin, Iran, Postal Code: 3431849689.
Phone: 02832232182
Fax: 02832225883
m.ebrahimian@kar.ac.ir

Article History
Received: 18 May 2025
Accepted: 5 June 2025
ePublished: 18 August 2025

ABSTRACT

For the torsion of nanotubes in nonlocal differential model, under uniform moment loading and linear moment loading along the nanotube as well as concentrated moment load at the free end, the solution is independent of scale parameter and chirality. While for nonlinear and sinusoidal moments, the solution depends on the scale and is independent of chirality. In this study, a new approach is applied using doublet mechanics (DM) where the governing equation are obtained using shell equilibrium equations and solved by angular displacement expansions with considering the scale parameter. With this approach, unlike the other methods, the effects of scale parameter and chirality are considered simultaneously. It is shown that angular displacement increases by increasing the scale parameter for different types of moment loading and boundary conditions. On the other hand, a Zigzag chirality has a lower torsional stiffness compared to an Armchair one. To validate the obtained result, the results of this work are compared with the nonlocal theory, integral nonlocal-finite element method (FEM) and molecular dynamics (MD) simulation results. Good agreement is observed specially with the two latter approaches.

Keywords: Scale parameter; Doublet mechanics; Chirality; Single-walled carbon nanotube; Torsion.

1 Introduction

In solid mechanics, in terms of mass distribution, two main models can be used, which include discrete and continuous models [1]. Engineering structures such as nanobeams, nanotubes, and nanospheres cannot be modeled with classical engineering relationships, and then a discrete model is needed for their analysis. scale parameter refers to the size range of materials being studied, typically measured in nanometers (nm), which is one billionth of a meter. Carbon nanotube was first discovered by Lijima in 1991 [2]. Single-walled carbon nanotubes (SWCNs) have unique properties highly dependent on their arrangement or chirality and their microscopic structure [1]. For this reason, a number of articles have investigated the effect of chirality on the properties of nanotubes using molecular methods [3-5] and shell model [6]. Because the local theory is a scale-independent theory, Eringen [7] used the non-local model of continuum mechanics and introduced the scale effect into the formulation.

The static and dynamic torsional behavior of circular nanosolids including nanotubes was studied based on the theory of non-local elastic stress field by Lee et al [8]. Their model presented different results in contrast to the traditional model that reported a reduction in hardness. Li [9] also presented the non-local shear stress field for torsional analysis of cylindrical nanostructures such as nanotubes, nanorods and nanoshafts and concluded that the torsional stiffness of nanostructures tend to get tough when the nonlocal effects are considered. Arda and Aydogdo [10] have investigated the static and dynamic torsion of carbon nanotubes (CNTs) located in an elastic bed using the theory of non-local elasticity. But the effects of scale and chirality in uniform and linear moments loading for nanotubes without elastic substrate did not appear. Lim et al. [11] developed a new nonlocal finite element method to solve the nonlocal integral equations of nanotubes in static and dynamic modes. Anyway, nonlocal theories are a simplified model without considering the properties of microstructures.

Molecular methods are among the most common methods in solving micromechanical problems. One of the most popular of them is molecular dynamics (MD) simulation. Predicting the mechanical properties of materials is one of the abilities of this method, which is done with proper accuracy. For this reason, many researchers have studied nanotube torsion using the MD method [12-15]. Xiong and Tian [16] found that by using MD simulation, Armchair nanotube shows better torsional resistance compared to Zigzag one. Wang et al. [17] simulated twisted carbon nanotubes by MD method and showed that the shear coefficient of carbon nanotubes increases with increasing radius of the tube. Yuji and Shijionobu [18] evaluated the torsional deformation of SWCNs using MD simulation. They realized that the torsional deformation results have a linear relationship between the torsional moment and the torsional angle per unit length. Among other molecular methods that solve the torsion problem is molecular structure mechanics [19]. Lasik et al. [4] used molecular mechanics models for SWCNs. They concluded that the torsion angle is small and decreases with the nanotube diameter. Anyway, MD simulation has a high volume of calculations despite the relatively appropriate accuracy, and for large systems, due to the presence of longitudinal dimensions in the nanoscale, it requires spending a lot of time and money.

Another model that researchers are interested in for analyzing the torsion of nanotubes is the shell model. Fuatta and Podioguidogli [6] investigated SWCNs with arbitrary chirality using the shell model, but did not use any scale parameters in their analysis. Khadem al-Hosseini et al [20] investigated the size effects in the torsional response of SWCNs by developing an improved nonlocal continuous shell model and also used MD simulation. Numerical methods such as finite elements [21] and meshless [22] are also another group of

methods used to investigate the torsion of nanotubes.

Another theory that has been of interest to researchers in recent years is DM. This theory was presented by Granik [1] and then developed by Granik and Farari [23]. DM presents a discrete physical model of solids, in which solids are defined as a set of points and nodes at definite or indefinite distances. Each pair of such nodes is known as a doublet. The use of micro-stresss and micro-strains is the basis of the DM method. DM equations have several major features. First, they are differential governing equations that make it easy to find a solution. Secondly, the governing equations include scale parameters explicitly. By using DM, chirality effects can be entered into the equations using the chiral angle but this method, like other nanoscale methods and theories, provides a non-scale solution for in a very limited number of loadings and boundary conditions, which can be improved using this method. Also, for greater accuracy, a larger number of terms of the scale parameter is required. Using these features, Ebrahimian et al. investigated the effects of scale parameter and chirality simultaneously in the bending of nanobeams [24] and the torsion of nanotubes [25]. Among the works done by DM on SWCNs, we can mention the vibrations of nanotubes [26-29] and nanotubes located in elastic bed [30]. Haghgoo et al. developed a two-step analytical model based on a percolation network model and electron tunneling theory to predict the electrical resistivity and percolation threshold of a hybrid nanocomposite system comprising carbon black (CB) and carbon nanotube (CNT) [31]. Noureddine et al. investigated the effect of chiral index and chiral angle dependent from diameter on vibration of SWCNTs using nonlocal Euler-Bernoulli beam model [32]. One of the applications of investigating the torsion problem of nanomaterials using the nonlocal method is to analyze and investigate the problem of cracking and damage. Modeling and analysis of fatigue life as well as the stress intensity factor in beams with cracks have also been investigated in [33 and 34]. On the other hand, the detection of damage and cracks in plate and cylindrical structures has also been investigated using new methods in [35 and 36].

Ebrahimian et al. analyzes the nonlinear coupled torsional-radial vibration of single-walled carbon nanotubes (SWCNTs) based on DM method and the results obtained with this method are compared with the fourth order Runge-Kuta numerical results and good agreement is observed [37]. Ebrahimian et al. delves into the nonlinear buckling behavior of a composite rectangular plate reinforced with graphene nanosheets, employing the third-order shear deformation principle. They understood the incorporation of graphene reinforcement notably enhanced the buckling load, with a mere 0.5% increase in graphene mass leading to a threefold rise in the buckling load [38]. In this paper, the torsion of the single-walled nanotubes is analyzed by using the shell balance equations in the cylindrical coordinate system with the help of DM, taking into account the effects of scale parameter and chirality explicitly. Also, a comparison should be made with the response of the nonlocal theory, which provides scale-independent responses for uniform, linear and concentrated moment loadings at the end of the nanotube. In any case, by using DM, the torsion analysis of nanotubes can be performed with proper accuracy, minimal assumptions in the governing equations and boundary conditions and also relatively less amount of calculations. On the other hand, this method is economical and time saving compared to MD simulation.

2 Brief review of DM

The structure of DM is based on a pair of geometrical or doublet nodes similar to what is shown in Figure 1. In doublets, it is possible that the relative separation of doublet nodes, the rotation of particles around the doublet axis, and the sliding of particles from their contact point, respectively cause microstrains of elongation ϵ_α, torsion μ_α and shear γ_α respectively.

In accordance with these microstrains, according to Figure 1, microstresses of elongational p_α, torsional m_α, and shear t_α can be defined. The first approximation of the relationship between microstresses and microstrains transforms the DM equations into Cauchy equations for nonpolar media and Causerat equations for polar media.
According to Figure 2, in the doublet (a, b_α), the vector ζ_α^0 that extends from the node a to b_α is called the doublet axis. The unit vector of this vector is denoted by τ_α^0. If $\eta_\alpha = |\zeta_\alpha^0|$ then $\tau_\alpha^0 = \frac{\zeta_\alpha^0}{\eta_\alpha}$. η_α is called scale parameter or doublet length.

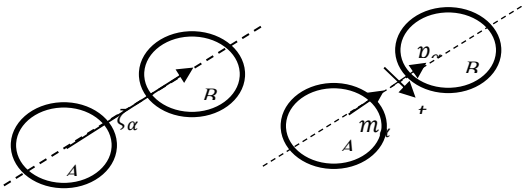

Figure 1- a doublet [26]

Using the simple geometry shown in Figure 2, microstrains can be expressed in terms of displacement vectors, rotations and their derivatives [1 transform to 37]. The equations in which the microstrains are expressed in terms of displacement and rotation vectors include the geometry of the network and internodal distances. Therefore, DM is a scaled theory.
In DM, it is assumed that each node has a vector of partial increase in rotation and displacement, which can be expanded as a convergent Taylor series around the network nodes. The order which this series is approximated is denoted by M. Approximation $M = 1$, which is referred to as a scale-free approximation, does not contain any information about the size of particles or distances between nodes which leads to classical continuum mechanics theory.

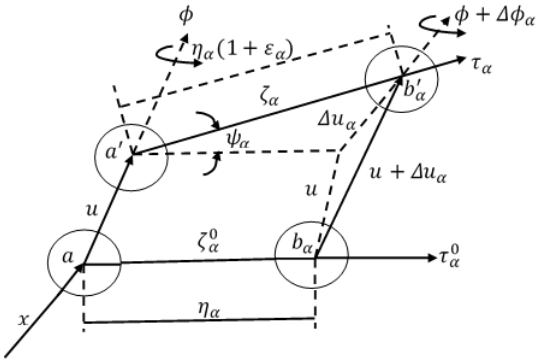

Figure 2- transition and rotation of the doublets

If in Figure 2, ζ_α^0 is the doublet axis in the initial state and ζ_α is the doublet axis in the transformed state, the following relationship is established:

$$\zeta_\alpha = \zeta_\alpha^0 + \Delta u_\alpha \quad (1)$$

In Eq. (1), $\alpha = 1,2,\dots,n$ denotes the number of doublet and Δu_α is the vector of partial displacement increase. If $u(X,t)$ of the displacement field represents the transfer from node a to its neighbor in Figure 2, then the partial increase vector Δu_α is written as follows:

$$\Delta u_\alpha = u(x + \zeta_\alpha^0, t) - u(x,t) \quad (2)$$

where x is the position vector of the particle
Eq. (2) can be expanded by Taylor convergent series around the neighborhood of arbitrary node a by approximating M.

$$\Delta u_\alpha = \sum_{\chi=1}^{M} \frac{\eta_\alpha^\chi}{\chi!} (\tau_\alpha^0 . \nabla)^\chi u(x,t) \quad (3)$$

In Eq. (3), the dot sign indicates the inner product and ∇ is the gradient operator in the general coordinate system.
We assume that the relative displacement between the nodes and the elongation microstrain in DM are small, that is, $\Delta u_\alpha \ll \eta_\alpha$ and $\epsilon_\alpha \ll 1$. With these assumptions, the angle ψ_α between τ_α and τ_α^0 in Figure 2 is very small, that is, $\psi_\alpha \ll 1$, so $\tau_\alpha^0 \approx \tau_\alpha$. So we have [1]:

$$\epsilon_\alpha = \frac{\tau_\alpha^0 . \Delta u_\alpha}{\eta_\alpha} \quad (4)$$

We put Eq. (3) in Eq. (4) which results to.

$$\epsilon_\alpha = \sum_{\chi=1}^{M} \frac{\eta_\alpha^{\chi-1}}{\chi!} \tau_\alpha^0 . (\tau_\alpha^0 . \nabla)^\chi u(x,t) \quad (5)$$

Eq. (5) expresses the relationship between axial microstrain in terms of displacement in DM. Using the definitions of microstresses based on strain energy and microstrains, as well as setting the first variation of the governing equation equal to zero for the medium with elastic microstructure, the following equations are obtained [1].

a) Linear momentum conservation equation:

$$\sum_{\alpha=1}^{n} \sum_{\chi=1}^{M} (-1)^{\chi-1} \frac{\eta_\alpha^{\chi-1}}{\chi!} (\tau_\alpha^0 . \nabla)^\chi (t_{\alpha i} + p_{\alpha i}) + F_i = \rho \frac{\partial^2 u_i}{\partial t^2} \quad (6)$$

b) Force boundary conditions at level S:

$$n_{k_r} \sum_{\alpha=1}^{n} \tau_{\alpha k_r}^0 \sum_{\chi=1}^{M} (-1)^{\chi-1} \frac{\eta_\alpha^{\chi-1}}{\chi!} (\tau_\alpha^0 . \nabla)^{\chi-r} (t_{\alpha i} + p_{\alpha i}) = T_i \delta_{r1} \quad (7)$$

In Eqs. (6) and (7), $\boldsymbol{n}$ is a vector perpendicular to the surface of S and δ_{r1} is Kronecker's delta. If M=1, then $r = 1$, but if $M \geq 2$, then $r = 1,2,\dots,M-1$. In any case, it must be $r+1 \leq \chi$, otherwise $\tau_{\alpha k_{r+1}}^0 \tau_{\alpha k_{r+2}}^0 \dots \tau_{\alpha k_\chi}^0 = 1$ and we ignore the differential expressions in Eq. (7), that is, $\partial^{\chi-r}(\dots) = (\dots)$.

In this article, we consider only the axially interaction between particles, that is, $p_\alpha \neq 0, m_\alpha = t_{\alpha i} = 0$. Assuming the same temperature and homogeneity of materials, the equation between axial microstress and axial microstrain is obtained as follows:

$$p_\alpha = \sum_{\beta=1}^{n} A_{\alpha\beta} \epsilon_\beta \quad (8)$$

In this equation, $A_{\alpha\beta}$ is the symmetric matrix of micromodules, which is a constant value for homogeneous materials. The matrix [A] contains the macroelastic constants obtained for a two-dimensional plane problem using Figure 3. In Figure 3, the coordinates of the plane are represented by $\theta_1 - \theta_2$ and we have only three pairs with the same angle of 120 degrees to each other.

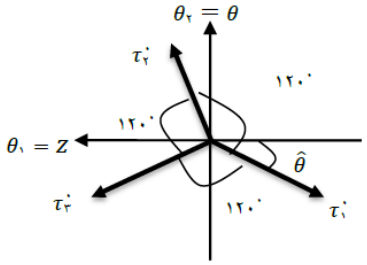

Figure 3. Three doublets with equal angles between them

For the two-dimensional and isotropic problem in DM, the matrix $[A]$ is a three-order symmetric matrix in the following general form [26]:

$$A = \begin{bmatrix} a & b & b \\ b & a & b \\ b & b & a \end{bmatrix} \quad (9)$$

It can be shown that the matrix coefficients [A] for isotropic materials are independent of direction [27]. In addition, the coefficients a and b under plane stress conditions are determined as follows.

$$a = \frac{4}{9}\mu \frac{7\lambda+10\mu}{\lambda+2\mu}, b = \frac{4}{9}\mu \frac{\lambda-2\mu}{\lambda+2\mu} \quad (10)$$

In Eq. (10), μ and λ are Lamé coefficients. In the case of plane stress, if b = 0, then the matrix [A] will be diagonal and the amount of calculations will be greatly reduced. This happens when λ=2μ or υ=1/3.

$$a = A_0 = \frac{8\mu}{3} = E \quad (11)$$

If we consider Eq. (8) for local interaction and non-polar environment, then micromoduli of elasticity will be $A_{\alpha\beta} = A_\alpha \delta_{\alpha\beta}$. If the local interaction is also homogeneous, i.e. the micromoduli of elasticity are the same for each pair, it can be assumed that $A_\alpha = A_0$. Therefore, Eq. (8) is reduced as follows:

$$p_\alpha = A_0 \epsilon_\alpha \quad (12)$$

3 Modeling SWCNs

SWCNs described as a single layer of graphite crystal wrapped into a seamless cylindrical shape.

The theoretical approach to nanotubes is formed by defining the indices relative to the lattice vectors on the hexagonal plane from which the tubes are formed. A tube is defined by defining a specific environment vector.

$$C = n_1 a_1 + n_2 a_2 \quad (13)$$

In Eq. (13), n_1 and n_2 are integers, a_1 and a_2 are lattice unit vectors and C is a chiral vector. It is possible to form a nanotube by mapping the origin to the point (n_1, n_2). Other parameters of SWCNs such as diameter $\widetilde{D}$ and chiral angle $\hat{\theta}$ can be calculated using n_1 and n_2 [3].

$$\widetilde{D} = \left(\frac{\sqrt{3}\eta}{\pi}\right)(n_2{}^2 + n_1 n_2 + n_1{}^2)^{1/2} \quad (14)$$

$$\hat{\theta} = \tan^{-1}\left(\frac{\sqrt{3}n_2}{n_2+2n_1}\right) \quad (15)$$

In these equations, η is the scale parameter in DM, which is considered equal to 0.142 nm for the carbon atom [26]. Due to the symmetry of the honeycomb network, i.e. $(n_1, n_2) = (n_2, n_1)$, the chiral angle $\hat{\theta}$ will be in the range of $0 \le \hat{\theta} \le 30$. If $n_2 = 0$, that is $(n_1, 0)$ or $\hat{\theta} = 0$, it is Zigzag and if $n_2 = n_1 = n$, that is (n, n) or $\hat{\theta} = 30$, it is Armchair and others The angles are called chiral [3].

4 DM model for macroshear stress equation in nanotube torsion

The surface force vector, T, is defined as follows:

$$T_i = \sigma_{ki} n_k \quad (16)$$

Using Eqs. (7) and (16), considering $r = 1$ and assuming the existence of axial microstress, the following equation is obtained:

$$\sigma_{ij}^{(M)} = \sum_{\alpha=1}^{n} \tau_{\alpha i}^0 \tau_{\alpha j}^0 \sum_{\chi=1}^{M} (-1)^{\chi-1} \frac{\eta_\alpha^{\chi-1}}{\chi!} (\tau_\alpha^0 . \nabla)^{\chi-1} p_\alpha \quad (17)$$

Eq. (17) is called macrostress equation in terms of microstress in DM theory and general coordinate system. By using Eqs. (5), (12) and (17), the macrostrain equation is obtained in terms of macrostress in DM for SWCNs that consist of three pairs with the same lengths and angles.

$$\sigma_{ij}^{(M)} = \sum_{\alpha=1}^{3} A_0 \tau_{\alpha i}^0 \tau_{\alpha j}^0 \left[\boldsymbol{\tau}_\alpha^0 . (\boldsymbol{\tau}_\alpha^0 . \boldsymbol{\varepsilon}) + \frac{\eta^2}{12}\left(\boldsymbol{\tau}_\alpha^0 . (\boldsymbol{\tau}_\alpha^0 . (\boldsymbol{\tau}_\alpha^0 . \boldsymbol{\nabla})(\boldsymbol{\tau}_\alpha^0 . \boldsymbol{\nabla}\boldsymbol{\varepsilon})\right)\right] \quad (18)$$

In Eq. (18), considering the cylindrical coordinate system shown in Figure 4, strain $\boldsymbol{\varepsilon}$, gradient operator $\boldsymbol{\nabla}$ and displacement $\boldsymbol{u}$ are defined as follows:

$$\boldsymbol{\varepsilon} = \frac{1}{2}\left((\boldsymbol{\nabla}\mathbf{u}) + (\boldsymbol{\nabla}\mathbf{u})^T\right) \quad (19)$$

$$\boldsymbol{\nabla} = \frac{\partial}{\partial r}\mathbf{e}_r + \frac{1}{r}\frac{\partial}{\partial \theta}\mathbf{e}_\theta + \frac{\partial}{\partial z}\mathbf{e}_z \quad (20)$$

$$\mathbf{u} = u_r \mathbf{e}_r + u_\theta \mathbf{e}_\theta + u_z \mathbf{e}_z \quad (21)$$

In this paper, Love's first approximation assumptions are considered:

- All points located on the line perpendicular to the middle plane will remain perpendicular after deformation, that is, transverse shear stresses $\sigma_{rz}^{(M)}$ and $\sigma_{r\theta}^{(M)}$ are ignored.
- Displacements are small compared to the shell thickness.
- The vertical stresses in the direction of the thickness $\sigma_{rr}^{(M)}$ are ignored, which is for plane stress.

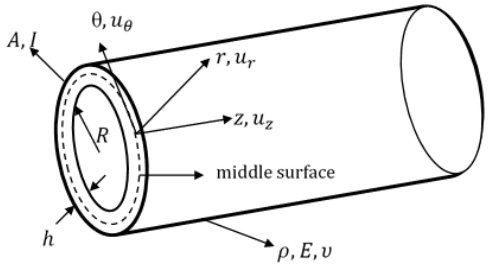

Figure 4- nanotube in cylindrical coordinate [28]

By studying the torsional deformation of homogeneous and uniform cylinders, it can be assumed that $u_r = u_z = 0$ and $u_\theta = u_\theta(z)$. In these assumptions, due to the very thin thickness of the SWCNs, changes in the direction of the radius have been ignored, and axial displacement has also been neglected. Due to axial symmetry $\frac{\partial}{\partial \theta} = 0$. According

to Figure 3, we can conclude that $\tau^0_{\alpha r}=0$. Therefore, the following relations are established:

$$\boldsymbol{\tau}^0_\alpha=\begin{bmatrix}0\\ \tau^0_{\alpha\theta}\\ \tau^0_{\alpha z}\end{bmatrix},\boldsymbol{\nabla}=\begin{bmatrix}\frac{\partial}{\partial r}\\ 0\\ \frac{\partial}{\partial z}\end{bmatrix},\boldsymbol{\nabla u}=\begin{bmatrix}0 & -\frac{u_\theta}{r} & 0\\ \frac{\partial u_\theta}{\partial r} & 0 & \frac{\partial u_\theta}{\partial z}\\ 0 & 0 & 0\end{bmatrix} \quad (22)$$

With the help of Eqs. (19) to (22) and the non-zero derivatives of the unit vectors in the cylindrical coordinate system, the terms of Eq. (18) can be obtained in terms of the only non-zero displacement, u_θ.

$$\sigma^{(M)}_{ij}=\sum_{\alpha=1}^{3}A_0\tau^0_{\alpha i}\tau^0_{\alpha j}\left[(\tau^0_{\alpha\theta})(\tau^0_{\alpha z})\frac{\partial u_\theta}{\partial z}+\frac{\eta^2}{12}\left(-\frac{3}{r^2}(\tau^0_{\alpha\theta})^3(\tau^0_{\alpha z})\frac{\partial u_\theta}{\partial z}+(\tau^0_{\alpha\theta})(\tau^0_{\alpha z})^3\frac{\partial^3 u_\theta}{\partial z^3}\right)\right] \quad (23)$$

Based on Love's assumptions for a one-dimensional elastic SWCN, the only non-zero shear stress component is obtained as follows:

$$\sigma^{(M)}_{\theta z}=\sum_{\alpha=1}^{3}A_0\left[(\tau^0_{\alpha\theta})^2(\tau^0_{\alpha z})^2\frac{\partial u_\theta}{\partial z}+\frac{\eta^2}{12}\left(-\frac{3}{r^2}(\tau^0_{\alpha\theta})^4(\tau^0_{\alpha z})^2\frac{\partial u_\theta}{\partial z}+(\tau^0_{\alpha\theta})^2(\tau^0_{\alpha z})^4\frac{\partial^3 u_\theta}{\partial z^3}\right)\right] \quad (24)$$

Considering Figure 3, the directors can be obtained along the length, radius and around the nanotube.

$$\tau^0_{1z}=-\cos\hat{\theta}\ ,\tau^0_{1\theta}=-\sin\hat{\theta}\ ,\tau^0_{1r}=0 \quad (25)$$

$$\tau^0_{2z}=\sin(30-\hat{\theta}),\tau^0_{2\theta}=\cos(30-\hat{\theta})\ ,\tau^0_{2r}=0 \quad (26)$$

$$\tau^0_{3z}=\cos(60-\hat{\theta}),\tau^0_{3\theta}=-\sin(60-\hat{\theta}),\tau^0_{3r}=0 \quad (27)$$

By putting Eqs. (25) to (27) in Eq. (24) and simplifying it, the following equation can be reached:

$$\sigma^{(M)}_{\theta z}=G\left[\frac{\partial u_\theta}{\partial z}+\frac{2\eta^2}{9}\left(-\frac{3}{r^2}f_1(\hat{\theta})\frac{\partial u_\theta}{\partial z}+f_2(\hat{\theta})\frac{\partial^3 u_\theta}{\partial z^3}\right)\right] \quad (28)$$

wherein

$$f_1(\hat{\theta})=\left((\sin\hat{\theta})^4(\cos\hat{\theta})^2\right)+\left((\cos(30-\hat{\theta}))^4(\sin(30-\hat{\theta}))^2\right)+\left((\sin(60-\hat{\theta}))^4(\cos(60-\hat{\theta}))^2\right) \quad (28\text{-a})$$

$$f_2(\hat{\theta})=\left((\sin\hat{\theta})^2(\cos\hat{\theta})^4\right)+\left((\cos(30-\hat{\theta}))^2(\sin(30-\hat{\theta}))^4\right)+\left((\sin(60-\hat{\theta}))^2(\cos(60-\hat{\theta}))^4\right) \quad (28\text{-b})$$

which in plane stress conditions $G=\frac{E}{2(1+\upsilon)}=\frac{3E}{8}=\frac{3A_0}{8}$. Eq. (28), in fact, is the shear macrostresss equation in a cylindrical coordinate system for a SWCN under the influence of torsion with the explicit consideration of the scale parameter and the chirality angle. It is clear that by setting the scale parameter equal to zero, the equation of local theory is obtained. It can also be seen that the classical equation is independent of chirality, while the DM equation is dependent on the angle between the doublets.

5 Shell equilibrium equations in DM

The general relationship for the result of forces N_{ij} and the result of moments M_{ij} is defined as follows based on terms of macrostresses [39] in DM:

$$N_{ij}=\int_{-\frac{h}{2}}^{\frac{h}{2}}\sigma^{(M)}_{ij}\,dr\ ,\quad M_{ij}=\int_{-\frac{h}{2}}^{\frac{h}{2}}\sigma^{(M)}_{ij}r\,dr \quad (29)$$

The equilibrium equations of the thin shell in cylindrical coordinates are obtained as follows [40]:

$$\frac{\partial N_{zz}}{\partial z}+\frac{1}{r}\frac{\partial N_{\theta z}}{\partial\theta}+\rho f_z=0 \quad (30)$$

$$\frac{\partial N_{z\theta}}{\partial z}+\frac{1}{r}\frac{\partial N_{\theta\theta}}{\partial\theta}+\frac{N_{\theta r}}{r}+\rho f_\theta=0 \quad (31)$$

$$\frac{\partial N_{zr}}{\partial z}+\frac{1}{r}\frac{\partial N_{\theta r}}{\partial\theta}-\frac{N_{\theta\theta}}{r}+\rho f_r=0 \quad (32)$$

$$\frac{\partial M_{zz}}{\partial z}+\frac{1}{r}\frac{\partial M_{\theta z}}{\partial\theta}+\rho l_z=N_{zr} \quad (33)$$

$$\frac{\partial M_{z\theta}}{\partial z}+\frac{1}{r}\frac{\partial M_{\theta\theta}}{\partial\theta}+\frac{M_{\theta r}}{r}+\rho l_\theta=N_{\theta r} \quad (34)$$

$$\frac{\partial M_{zr}}{\partial z}+\frac{1}{r}\frac{\partial M_{\theta r}}{\partial\theta}-\frac{M_{\theta\theta}}{r}+\rho l_r=N_{rr} \quad (35)$$

In Eqs. (30) to (35), ρ, f, and l are the mass density, force density, and couple per unit mass of the surface, respectively.

6 The governing equation for torsion of nanotubes

With the Taylor expansion of Eq. (28), around the middle surface, the second terms of the expansion can be omitted due to the small thickness in the nanotube. Finally, by putting Eq. (28) into Eq. (29), the following relations are obtained:

$$N_{\theta z} = Gh\left[\frac{\partial u_\theta}{\partial z} + \frac{2\eta^2}{9}\left(-\frac{3}{R^2}f_1(\hat{\theta})\frac{\partial u_\theta}{\partial z} + f_2(\hat{\theta})\frac{\partial^3 u_\theta}{\partial z^3}\right)\right] \quad (36\text{-a})$$

$$M_{\theta z} = 0 \quad (36\text{-b})$$

According to the assumptions mentioned in section 2 and Eqs. (36), Eqs. (30) to (35) are reduced to the following equations:

$$\frac{\partial N_{\theta z}}{\partial z} + \rho f_\theta = 0 \quad , \frac{\partial M_{\theta z}}{\partial z} + \rho l_\theta = 0 \quad (37)$$

By inserting Eqs. (36) into Eqs. (37) and the relation $u_\theta = R\phi$ where ϕ is the angular displacement, the following equation is obtained:

$$GI_P\left[\frac{\partial^2\phi}{\partial z^2} + \frac{2\eta^2}{9}\left(-\frac{3}{R^2}f_1(\hat{\theta})\frac{\partial^2\phi}{\partial z^2} + f_2(\hat{\theta})\frac{\partial^4\phi}{\partial z^4}\right)\right] + T = 0 \quad (38)$$

In Eq. (38), I_P is the polar moment obtained for the circular cross section of the thin wall from the relation $I_P = 2\pi R^3 h$ and T is the moment per unit length. Eq. (38) is actually the governing equation for torsion of SWCN considering chirality and the scale parameters at the same time. For the torsion problem of thin tubes, the product of the shear stress by the thickness is always a constant number. Therefore, the torsional moment in DM is calculated as follows:

$$T_t = \int \sigma_{\theta z}^{(M)} hrds = 2A_m h\sigma_{\theta z}^{(M)} \quad (39)$$

In Eq. (39), $A_m = \pi R^2$ is the area created by the cross section of the middle layer. Therefore, by replacing Eq. (28) in Eq. (39), the following relationship is obtained:

$$T_t = GI_P\left[\frac{\partial\phi}{\partial z} + \frac{2\eta^2}{9}\left(-\frac{3}{R^2}f_1(\hat{\theta})\frac{\partial\phi}{\partial z} + f_2(\hat{\theta})\frac{\partial^3\phi}{\partial z^3}\right)\right] \quad (40)$$

It is also clear in this equation that by setting the scale parameter equal to zero, the classic equation of torsional moment is obtained.

7 Single-walled nanotube under uniform moment load

In this case, the uniform moment load is defined as $T = T_0$. Therefore, Eq. (38) is rewritten as follows:

$$GI_P\left[\frac{\partial^2\phi}{\partial z^2} + \frac{2\eta^2}{9}\left(-\frac{3}{R^2}f_1(\hat{\theta})\frac{\partial^2\phi}{\partial z^2} + f_2(\hat{\theta})\frac{\partial^4\phi}{\partial z^4}\right)\right] + T_0 = 0 \quad (41)$$

According to the solution of the problems by the DM method, the angular displacement can be expanded as follows:

$$\phi = \phi_0 + \eta\phi_1 + \eta^2\phi_2 \quad (42)$$

In Eq. (42), ϕ_0 is the angular displacement in classical elasticity, and ϕ_1 and ϕ_2 refer to the angular displacements under the influence of the scale parameter. By inserting Eq. (42) into Eq. (41) and sorting it based on the first three powers of η, the following equations are obtained:

$$\eta^0 \Rightarrow \frac{\partial^2\phi_0}{\partial z^2} = -\frac{T_0}{GI_P} \quad (43\text{-a})$$

$$\eta^1 \Rightarrow \frac{\partial^2\phi_1}{\partial z^2} = 0 \quad (43\text{-b})$$

$$\eta^2 \Rightarrow \frac{\partial^2\phi_2}{\partial z^2} - \frac{2f_1(\hat{\theta})}{3R^2}\frac{\partial^2\phi_0}{\partial z^2} + \frac{2f_2(\hat{\theta})}{9}\frac{\partial^4\phi_0}{\partial z^4} = 0 \quad (43\text{-c})$$

To make the governing equations dimensionless, the following definitions are used:

$$\bar{z} = \frac{z}{L} \quad , \quad \bar{\phi} = \phi\frac{GI_P}{T_0L^2} \quad , \quad \bar{\phi} = \phi\frac{GI_P}{T_1L} \quad (44)$$

In these relations, T_0 and T_1 are respectively the spread moment load along the length of the nanotube and the concentrated moment load at the free end of the nanotube.

Clamped-clamped boundary condition

For the two ends clamped boundary condition, the angular displacement at both ends of the nanotube is zero. Therefore, considering Eq. (42), the following boundary conditions are established at $z = 0$ and $z = L$:

$$\eta^0 \Rightarrow \phi_0 = 0 \ , \ \eta^1 \Rightarrow \phi_1 = 0 \ , \ \eta^2 \Rightarrow \phi_2 = 0 \quad (45)$$

By solving Eqs. (43) with the help of boundary conditions (45) and applying definitions (44), the following relationship is obtained:

$$\bar{\phi}^{(\mathrm{DM})} = \left(-\frac{\bar{z}^2}{2} + \frac{\bar{z}}{2}\right) + \frac{\eta^2 f_1(\hat{\theta})}{3R^2}(-\bar{z}^2 + \bar{z}) \qquad (46)$$

In Eq. (46), for the first time, chirality and scale effects are simultaneously and explicitly considered for the torsion problem of single-walled nanotube under uniform moment load and double clamped end boundary conditions. By setting η=0, the local theory solution is obtained. For this problem, the nonlocal theory [10, 11] provides a scale-free solution and is unable to consider the effects of the angle between doublets and the scale parameter. Eq. (46) for Zigzag and Armchair is obtained as follows:

$$\hat{\theta} = 0 \Longrightarrow \bar{\phi}^{(\mathrm{DM})}_{\mathrm{Zigzag}} = -\frac{\bar{z}^2}{2} + \frac{\bar{z}}{2} + \frac{3\eta^2}{32R^2}(-\bar{z}^2 + \bar{z}) \quad (47)$$

$$\hat{\theta} = 30 \Longrightarrow \bar{\phi}^{(\mathrm{DM})}_{\mathrm{Armchair}} = -\frac{\bar{z}^2}{2} + \frac{\bar{z}}{2} + \frac{\eta^2}{32R^2}(-\bar{z}^2 + \bar{z}) \quad (48)$$

By observing Eqs. (47) and (48), it can be concluded that the amount of angular displacement of Zigzag and Armchair increases compared to the classical case, that is, DM in the scaled state produces a softer nanotube than the local state. The result obtained from DM is different from the nonlocal theory [10, 11] and agrees with the prediction of the integral nonlocal finite element method [11].
From the comparison between Eqs. (47) and (48), it is clear that Armchair nanotube is harder than Zigzag one. It can also be concluded that as much as the scale parameter is important, chirality is also important and affects the behavior of nanotubes.

Clamped-free Boundary condition
For this boundary condition, the same boundary condition (45) is established at $z = 0$. But at the free end at z=L, taking the derivative of Eq. (42) and setting it equal to zero, the following boundary conditions are obtained:

$$\eta^0 \Rightarrow \frac{\partial \phi_0}{\partial z} = 0 \ , \ \eta^1 \Rightarrow \frac{\partial \phi_1}{\partial z} = 0 \ , \ \eta^2 \Rightarrow \frac{\partial \phi_2}{\partial z} = 0 (94)$$

By solving Eqs. (43) with the help of boundary conditions (45) and (49) and using definitions (44), the following result is obtained:

$$\bar{\phi}^{(\mathrm{DM})} = \left(-\frac{\bar{z}^2}{2} + \bar{z}\right) + \frac{\eta^2 f_1(\hat{\theta})}{3R^2}(-\bar{z}^2 + 2\bar{z}) \qquad (50)$$

While the nonlocal theory [10, 11] for the clamped-free boundary condition also provides solutions independent of the chirality and scale parameters, in Eq. (50) these parameters exist explicitly and simultaneously. Eq. (50) for Zigzag and Armchair is as follows:

$$\hat{\theta} = 0 \Longrightarrow \bar{\phi}^{(\mathrm{DM})}_{\mathrm{Zigzag}} = -\frac{\bar{z}^2}{2} + \bar{z} + \frac{3\eta^2}{32R^2}(-\bar{z}^2 + 2\bar{z}) (51)$$

$$\hat{\theta} = 30 \Longrightarrow \bar{\phi}^{(\mathrm{DM})}_{\mathrm{Armchair}} = -\frac{\bar{z}^2}{2} + \bar{z} + \frac{\eta^2}{32R^2}(-\bar{z}^2 + 2\bar{z}) (52)$$

As it is clear from the Eqs. (51) and (52), DM predicts the softening of the nanotube in both the Zigzag and Armchair states in the clamped-free boundary condition compared to the local or classical case. This prediction agrees with the integral nonlocal finite element method [11].
Also, in this case, the angular displacement of the Zigzag nanotube is more than that of the Armchair. Therefore, it can be concluded that in both double ends clamped and single end clamped boundary conditions, according to the prediction of DM, the change of chirality from 0 to 30 degrees creates a harder nanotube. This issue determines the importance of chirality effect.

8 Single-walled nanotube under linear moment load

In this part of the present work, the linear moment load $T = T_0 {}^{z}/_{L}$ is considered and Eq. (38) is written as follows:

$$GI_P\left[\frac{\partial^2 \phi}{\partial z^2} + \frac{2\eta^2}{9}\left(-\frac{3}{R^2} f_1(\hat{\theta})\frac{\partial^2 \phi}{\partial z^2} + f_2(\hat{\theta})\frac{\partial^4 \phi}{\partial z^4}\right)\right] + T_0 {}^{z}/_{L} = 0 \qquad (53)$$

Eq. (42) is placed in Eq. (53):

$$\eta^0 \Rightarrow \frac{\partial^2 \phi_0}{\partial z^2} = -\frac{T_0 z}{GI_P L} \qquad (54\text{-a})$$

$$\eta^1 \Rightarrow \frac{\partial^2\phi_1}{\partial z^2} = 0 \quad (54\text{-b})$$

$$\eta^2 \Rightarrow \frac{\partial^2\phi_2}{\partial z^2} - \frac{2f_1(\hat{\theta})}{3R^2}\frac{\partial^2\phi_0}{\partial z^2} + \frac{2f_2(\hat{\theta})}{9}\frac{\partial^4\phi_0}{\partial z^4} = 0 \quad (54\text{-c})$$

Two ends clamped boundary condition

By solving Eq. (54) using boundary conditions (45) at $z = 0, L$ and applying definitions (44), the following result is obtained:

$$\bar{\phi}^{(DM)} = \left(-\frac{\bar{z}^3}{6} + \frac{\bar{z}}{6}\right) + \frac{\eta^2 f_1(\hat{\theta})}{9R^2}(-\bar{z}^3 + \bar{z}) \quad (55)$$

By setting the scale parameter equal to zero, the solutions of local and nonlocal theories [10], which are also independent of the chiral angle, are obtained. By changing the chiral angle, the angular displacement for two Zigzag and Armchair arrangements can be obtained as follows:

$$\hat{\theta} = 0 \Longrightarrow \bar{\phi}^{(DM)}_{Zigzag} = -\frac{\bar{z}^3}{6} + \frac{\bar{z}}{6} + \frac{\eta^2}{32R^2}(-\bar{z}^3 + \bar{z}) \quad (56)$$

$$\hat{\theta} = 30 \Longrightarrow \bar{\phi}^{(DM)}_{Armchair} = -\frac{\bar{z}^3}{6} + \frac{\bar{z}}{6} + \frac{\eta^2}{96R^2}(-\bar{z}^3 + \bar{z}) \quad (57)$$

Clamped-free boundary condition

By solving Eqs. (54) with the help of boundary conditions (45) at z=0 and (49) at z=L and using definitions (44), the following result is obtained:

$$\bar{\phi}^{(DM)} = \left(-\frac{\bar{z}^3}{6} + \frac{\bar{z}}{2}\right) + \frac{\eta^2 f_1(\hat{\theta})}{9R^2}(-\bar{z}^3 + 3\bar{z}) \quad (58)$$

Eq. (58) also depends on both chirality and scale parameters, unlike the nonlocal theory [10]. For Zigzag and Armchair, Eq.n (58) is reduced as follows:

$$\hat{\theta} = 0 \Longrightarrow \bar{\phi}^{(DM)}_{Zigzag} = -\frac{\bar{z}^3}{6} + \frac{\bar{z}}{2} + \frac{\eta^2}{32R^2}(-\bar{z}^3 + 3\bar{z}) \quad (59)$$

$$\hat{\theta} = 30 \Longrightarrow \bar{\phi}^{(DM)}_{Armchair} = -\frac{\bar{z}^3}{6} + \frac{\bar{z}}{2} + \frac{\eta^2}{96R^2}(-\bar{z}^3 + 3\bar{z}) \quad (60)$$

As it is clear from Eqs. (55) to (60), DM in linear moment load also provides scale-dependent responses for different chirality. Also, the equations show that, similar to the uniform moment load, for both one-end and two-end clamped boundary conditions, the Armchair has more torsional stiffness than the Zigzag.

9 Single-walled nanotube under concentrated load at the end

In this case, the concentrated moment load enters the problem through boundary conditions. Therefore, Eq. (38) is reduced as follows:

$$GI_P\left[\frac{\partial^2\phi}{\partial z^2} + \frac{2\eta^2}{9}\left(-\frac{3}{R^2}f_1(\hat{\theta})\frac{\partial^2\phi}{\partial z^2} + f_2(\hat{\theta})\frac{\partial^4\phi}{\partial z^4}\right)\right] = 0 \quad (61)$$

Using Eqs. (42) and (61), the governing equation based on the power of the scale parameter can be regularized as follows:

$$\eta^0 \Rightarrow \frac{\partial^2\phi_0}{\partial z^2} = 0 \quad (62\text{-a})$$

$$\eta^1 \Rightarrow \frac{\partial^2\phi_1}{\partial z^2} = 0 \quad (62\text{-b})$$

$$\eta^2 \Rightarrow \frac{\partial^2\phi_2}{\partial z^2} - \frac{2f_1(\hat{\theta})}{3R^2}\frac{\partial^2\phi_0}{\partial z^2} + \frac{2f_2(\hat{\theta})}{9}\frac{\partial^4\phi_0}{\partial z^4} = 0 \quad (62\text{-c})$$

Clamped-free boundary condition

In this case, one end at $z = 0$ is kept fixed and the other end at $z = L$ is twisted. Therefore, the boundary conditions (45) prevail at the fixed end. Using Eqs. (40) and (42), the boundary conditions at the free end are determined as follows:

$$\eta^0 \Rightarrow \frac{\partial\phi_0}{\partial z} = \frac{T_1}{GI_P} \quad (63\text{-a})$$

$$\eta^1 \Rightarrow \frac{\partial\phi_1}{\partial z} = 0 \quad (63\text{-b})$$

$$\eta^2 \Rightarrow \frac{\partial\phi_2}{\partial z} - \frac{2f_1(\hat{\theta})}{3R^2}\frac{\partial\phi_0}{\partial z} + \frac{2f_2(\hat{\theta})}{9}\frac{\partial^3\phi_0}{\partial z^3} = 0 \quad (63\text{-c})$$

By solving Eqs. (62) with boundary conditions (45) and (63) and using definitions (44), the following relationship is obtained:

$$\bar{\phi}^{(DM)} = \bar{z} + \frac{2\eta^2 f_1(\hat{\theta})}{3R^2}\bar{z} \quad (64)$$

For Zigzag and Armchair arrangements, the following equations are calculated:

$$\hat{\theta} = 0 \Longrightarrow \bar{\phi}^{(DM)}_{Zigzag} = \bar{z} + \frac{3\eta^2}{16R^2}\bar{z} \quad (65)$$

$$\hat{\theta} = 30 \Longrightarrow \bar{\phi}^{(DM)}_{Armchair} = \bar{z} + \frac{\eta^2}{16R^2}\bar{z} \quad (66)$$

According to Eqs. (64) to (66), it is clear that the response of DM, unlike the nonlocal theory [11], depends on both chirality and scale parameters.

Also, the angular displacement similar to the prediction of the integral finite element method [11] has increased compared to the classical case. In this loading, it has been shown that according to the prediction of DM in other loadings, Armchair nanotube is harder than Zigzag due to less angular displacement.

10 Numerical results and discussion

In this section, the numerical results for the torsion of single-walled nanotubes are presented. The results obtained from DM are compared with the results of local theory, nonlocal theory [10, 11], integral nonlocal finite element method [11] and MD simulation [20]. Because it has been proven that the MD simulation method is very close to the experimental method, this paper compares DM with MD [20]. Zigzag (10, 0) and Armchair (6, 6) nanotubes with the specifications presented in Table 1 are considered.

Table 1- specification of Zigzag (10, 0) and Armchair (6, 6)

Chirality	nanotube specification [20]		
	G. h($^{nN}/_{nm}$)	(nm) length	(nm) diameter
(10, 0)	136.15	12.20	0.775
(6, 6)	153.17	11.84	0.805

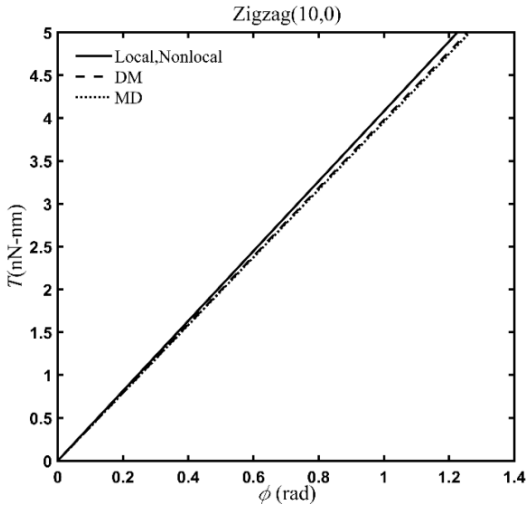

(a)

In order to verify the validity of the present work, in Figure 5, the DM results are compared with the results obtained from local and nonlocal theories and MD simulation for Zigzag and Armchair SWCNs. The torsional moment is considered to be 5 nN.nm. A good agreement has been obtained between the results of MD simulation and the present work. It can be seen that DM and MD simulation [20] for Zigzag and Armchair cases predict the softening of SWCNs compared to the classical state while the nonlocal theory corresponds to the local theory.

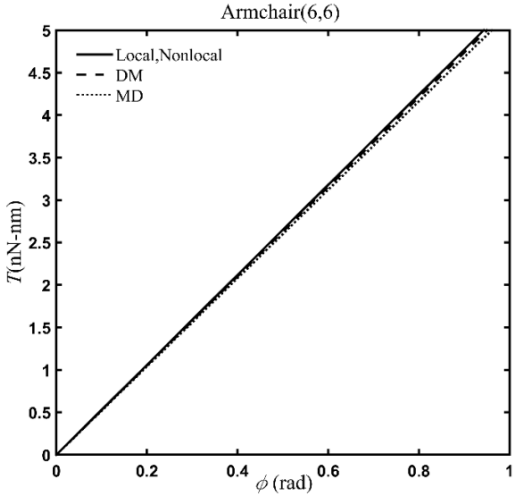

(b)

Figure 5- Comparison of molecular dynamics (MD) and doublet mechanics (DM) simulation results for (a) Zigzag and (b) Armchair SWCNs

For another comparison, in Figure 6, the results of DM are compared with the integral nonlocal finite element method [11] for two-ends and one-end clamped boundary conditions under uniform moment load and concentrated moment load at the end. The method of integral nonlocal finite elements and DM in all cases predicts an increase in angular displacement compared to the local theory.

It is also clear that the angular displacement of Zigzag is always more than Armchair, and this means that Armchair is generally harder than Zigzag with the same dimensions. This result agrees with the prediction of MD simulation [16, 38] and finite element method [3]. In Figure 6, $\mu = (e_0 a)^2$ is the nonlocal scale parameter in the integral nonlocal finite element method.

In Figure 7, the effect of chirality on the dimensionless angular displacement of nanotubes under the torsion influence has been investigated. As can be seen, in all cases, with the change of the chiral angle from 0 to 30 degrees, in various scale parameters, the value of the dimensionless angular displacement decreases. This issue once again shows that zigzag is softer than armchair. It is also clear that the classical state $\eta = 0$ is independent of the chiral angle change.

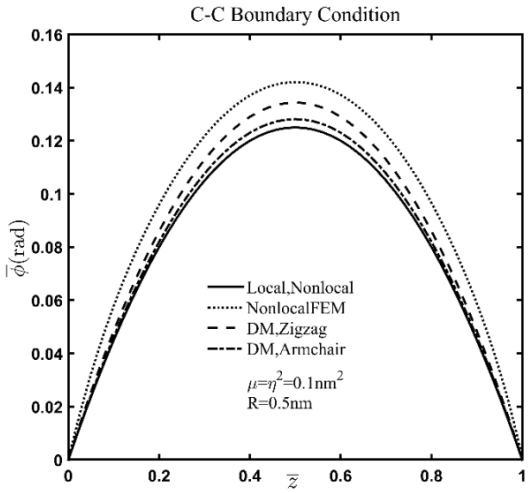

(a)

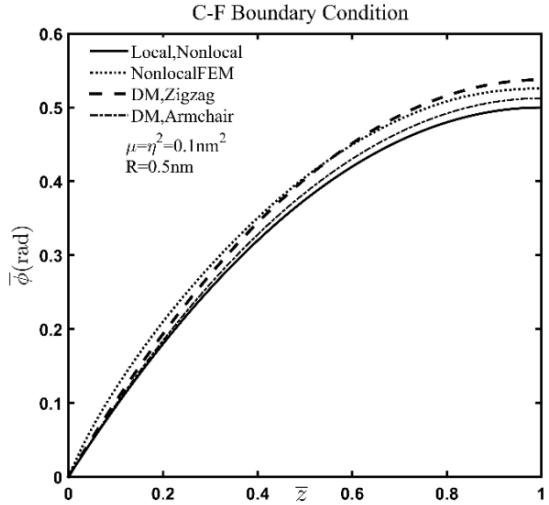

(b)

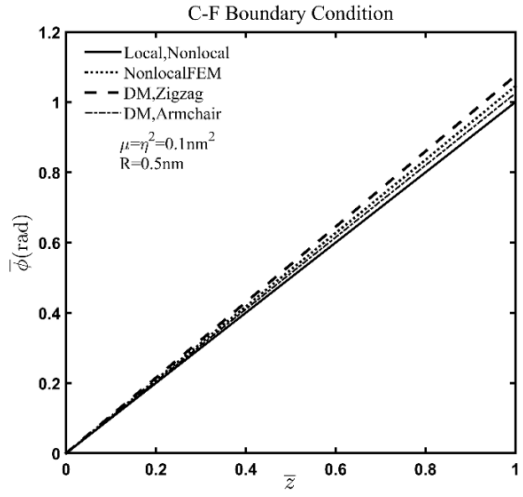

(c)

Figure 6- Comparison of the results of integral nonlocal finite elements and duablet mechanics (DM) for nanotubes (a) and (b) uniform moment load (c) concentrated moment load at the free end

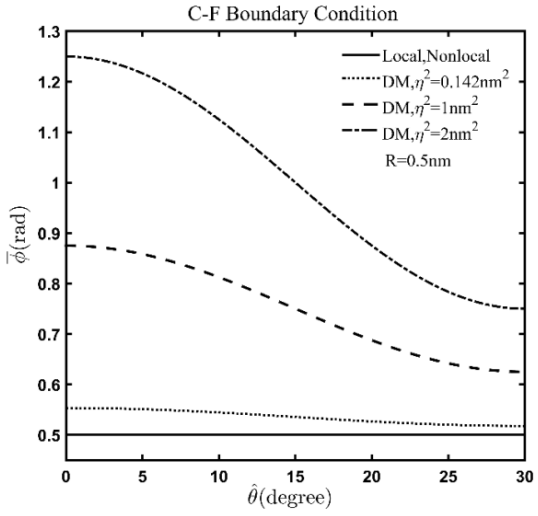

(a)

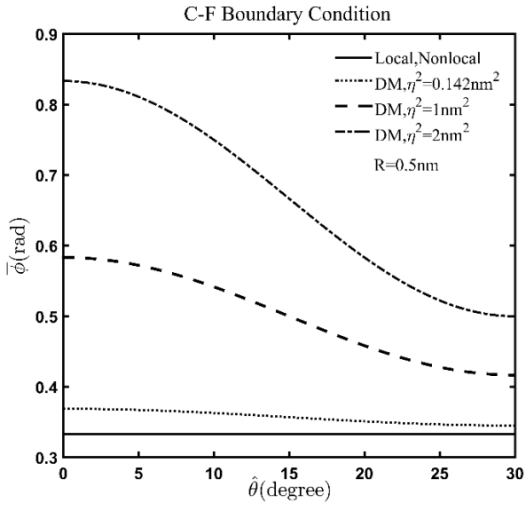

(b)

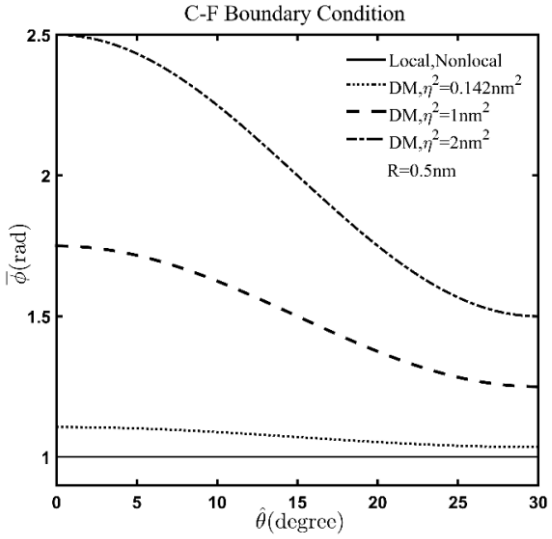

(c)

Figure 7- Chirality effects on nanotubes under (a) uniform moment load (b) linear moment load (c) concentrated moment at the free end

In Figure 8, the effect of the scale parameter on the dimensionless angular displacement for nanotubes is investigated. The dimensionless angular displacement of DM for zigzag and armchair is

larger than the local dimensionless angular displacement. While the nonlocal dimensionless angular displacement corresponds to its local value and the nonlocal theory provides a scale-independent response, DM predicts the softening of the nanotube as the scale parameter increases.

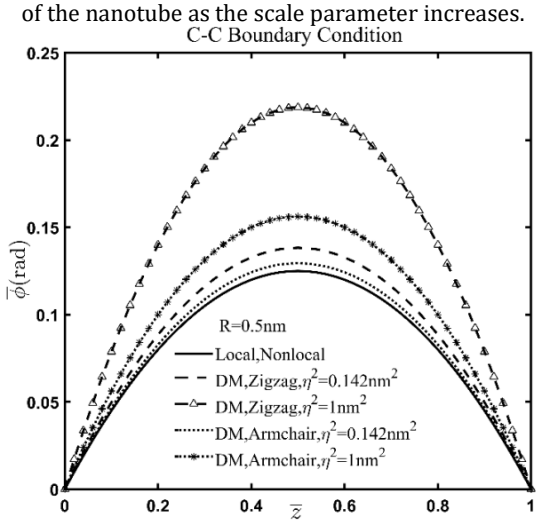

(a)

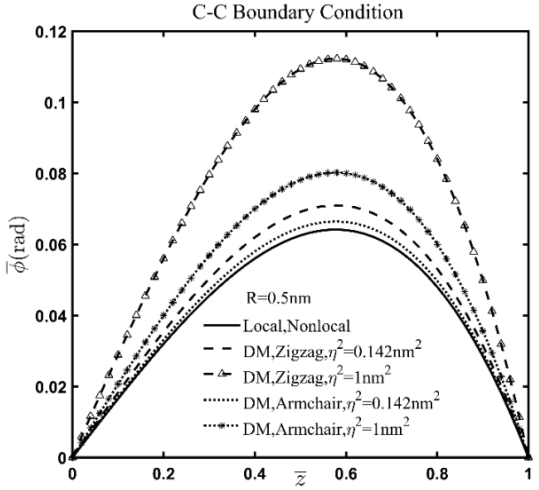

(c)

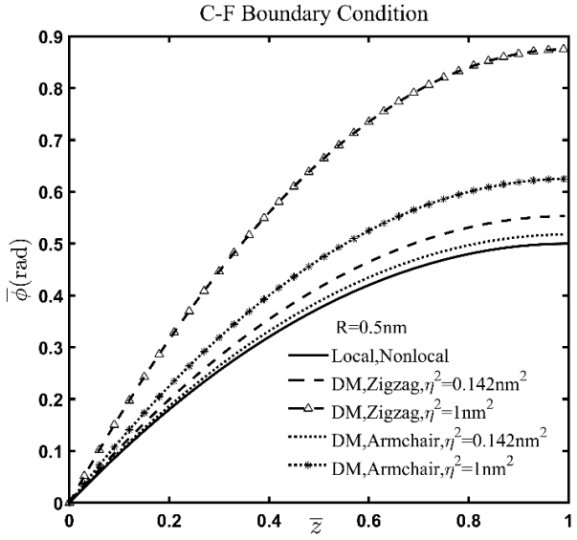

(b)

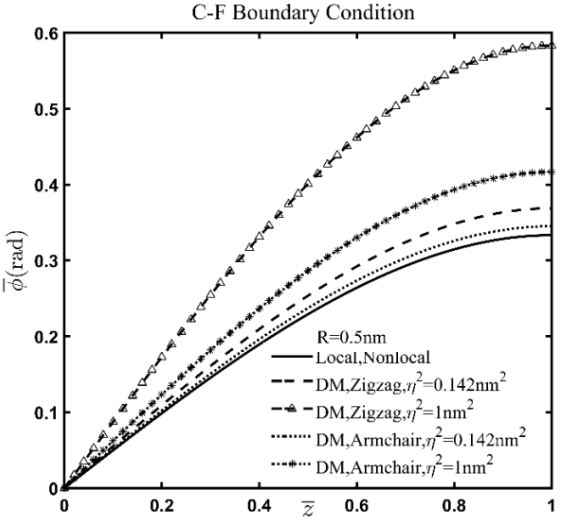

(d)

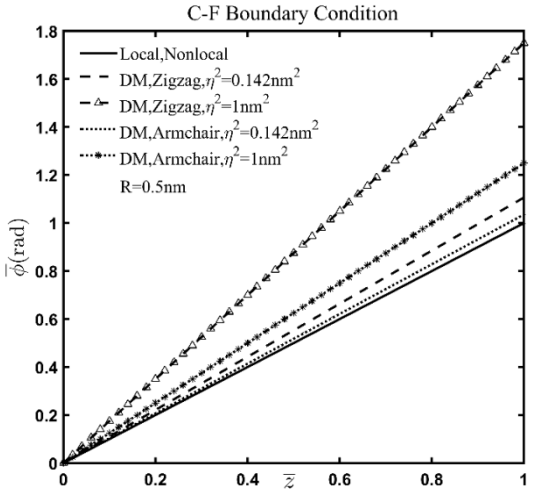

(e)

Figure 8- Scale parameter effects on nanotubes (a) and (b) uniform moment load (c) and (d) linear moment load (e) concentrated moment load at the free end

11 Summary and conclusion

In this paper, the static torsion of nanotubes has been investigated. The governing equations have been obtained by using the shell equilibrium and DM equations and have been solved by expanding the angular displacement based on scale parameter terms for different boundary conditions. The following results have been obtained:

1. If the scale properties are important in the analysis of nanotubes, the chirality effect is equally important. Therefore, the chiral angle should be considered in the calculations. This fact is clearly shown by DM.

2. An analytical response dependent on the scale effect and chiral angle is provided for the torsion of nanotubes. While the differential nonlocal theory for uniform, linear and concentrated moment loadings at the end results in scale free responses.

3. Dimensionless angular displacement for nanotubes under uniform, linear and concentrated moment load at the end and various boundary conditions increases with the increase of the scale parameter and shows the softening of the nanotube. This prediction agrees with the results of integral nonlocal finite element method and MD simulation. While the prediction of nonlocal differential and local theories coincide and are independent of chirality and scale parameter.
4. Angular displacement decreases with increasing chiral angle. Also, the angular displacement of Zigzag is more than that of Armchair for various types of loads and boundary conditions. In other words, Armchair nanotube has more torsional stiffness compared to Zigzag. These results are confirmed by MD simulation.

12 Disclosure of Potential Conflicts of Interest

The Authors declare that there is no conflict of interest

13 Reference

[1] M. Ferrari, V. T. Granik, A. Imam, and J. C. Nadeau, Advances in Doublet Mechanics. Springer-Verlag, Berlin Heidelberg, 1997.

[2] H.-T. Thai, "A nonlocal beam theory for bending, buckling, and vibration of nanobeams," International Journal of Engineering Science, vol. 52, pp. 56-64, 3// 2012.

[3] M. Zakeri and M. Shayanmehr, "On the Mechanical Properties of Chiral Carbon Nanotubes," Journal of Ultrafine Grained and Nanostructured Materials, vol. 46, no. 1, pp. 1-9, 2013.

[4] N. Lazić, T. Vuković, G. Volonakis, I. Milošević, S. Logothetidis, and M. Damnjanović, "Natural torsion in chiral single-wall carbon nanotubes," Journal of Physics: Condensed Matter, vol. 24, no. 48, p. 485302, 2012.

[5] G. Cao and X. Chen, "The effects of chirality and boundary conditions on the mechanical properties of single-walled carbon nanotubes," International Journal of Solids and Structures, vol. 44, no. 17, pp. 5447-5465, 8/15/ 2007.

[6] A. Favata and P. Podio-Guidugli, "A shell theory for chiral single-wall carbon nanotubes," European Journal of Mechanics - A/Solids, vol. 45, pp. 198-210, 5// 2014.

[7] A. C. Eringen, "Nonlocal polar elastic continua," International Journal of Engineering Science, vol. 10, no. 1, pp. 1-16, 1972/01/01 1972.

[8] C. Li, C. W. Lim, and J. Yu, "Torsion statics and dynamics for circular elastic nanosolids by nonlocal elasticity theory," Acta Mechanica Solida Sinica, vol. 24, no. 6, pp. 484-494, 2011/12/01 2011.

[9] C. Li, "A nonlocal analytical approach for torsion of cylindrical nanostructures and the existence of higher-order stress and geometric boundaries," Composite Structures, vol. 118, pp. 607-621, 12// 2014.

[10] M. Arda and M. Aydogdu, "Torsional statics and dynamics of nanotubes embedded in an elastic medium," Composite Structures, vol. 114, pp. 80-91, 8// 2014.

[11] C. W. Lim, M. Z. Islam, and G. Zhang, "A nonlocal finite element method for torsional statics and dynamics of circular nanostructures," International Journal of Mechanical Sciences, vol. 94–95, pp. 232-243, 5// 2015.

[12] Q. W. Zhang and B. Li, "Torsional behavior of single-walled carbon nanotubes," Carbon, vol. 94, pp. 826-835, 11// 2015.

[13] M.-J. Chen, Y.-C. Liang, H.-Z. Li, and D. Li, "Molecular dynamics simulation on mechanical property of carbon nanotube torsional deformation," Chinese Physics, vol. 15, no. 11, p. 2676, 2006.

[14] A. I. Melker and A. I. Zhaldybin, "Molecular Dynamics Study of Torsion of Single-Wall Carbon Nanotubes," Physics,, Chemistry and Application of Nanostructures, pp. 233-236, 2007.

[15] Z. Wang, M. Devel, and B. Dulmet, "Torsion carbon nanotubes: A molecular dynamics study," Surface Science, vol. 604, no. 5–6, pp. 496-499, 3/15/ 2010.

[16] Q.-l. Xiong and X. G. Tian, "Torsional properties of hexagonal boron nitride nanotubes, carbon nanotubes and their hybrid structures: A molecular dynamics study," AIP Advances, vol. 5, no. 10, p. 107215, 2015.

[17] Y. Wang, X. Wang Xiu, and X. Ni, "Atomistic simulation of the torsion deformation of carbon nanotubes," Modelling and Simulation in Materials Science and Engineering, vol. 12, no. 6, p. 1099, 2004.

[18] S. Yoji and O. Shigenobu, "Mechanical integrity of carbon nanotubes for bending and torsion," Modelling and Simulation in Materials Science and Engineering, vol. 12, no. 4, p. 599, 2004.

[19] R. Merli, C. Lázaro, S. Monleón, and A. Domingo, "A molecular structural mechanics model applied to the static behavior of single-walled carbon nanotubes: New general formulation," Computers & Structures, vol. 127, pp. 68-87, 10// 2013.

[20] F. Khademolhosseini, R. K. N. D. Rajapakse, and A. Nojeh, "Torsional buckling of carbon nanotubes based on nonlocal elasticity shell models," Computational Materials Science, vol. 48, no. 4, pp. 736-742, 6// 2010.

[21] A. F. G. Pereira, J. V. Fernandes, J. M. Antunes, and N. A. Sakharova, "Shear modulus and Poisson's ratio of single-walled carbon nanotubes: Numerical evaluation," Phys. Status Solidi B, vol. 253, pp. 366–376, 2016.

[22] Y. Sun and K. M. Liew, "Mesh-free simulation of single-walled carbon nanotubes using higher order Cauchy–Born rule," Computational Materials Science, vol. 42, no. 3, pp. 444-452, 5// 2008.

[23] V. T. Granik and M. Ferrari, "Microstructural mechanics of granular media," Mechanics of Materials, vol. 15, no. 4, pp. 301-322, 1993.

[24] M. R. Ebrahimian, A. Imam, and M. Najafi, "Doublet mechanical analysis of bending of Euler-Bernoulli and Timoshenko nanobeams," ZAMM - Journal of Applied Mathematics and Mechanics / Zeitschrift für Angewandte Mathematik und Mechanik, vol. 98, no. 9, pp. 1642-1665, 2018/09/01 2018.

[25] M. R. Ebrahimian, A. Imam, and M. Najafi, "The effect of chirality on the torsion of nanotubes embedded in an elastic medium using doublet mechanics," Indian Journal of Physics, vol. 94, no. 1, pp. 31-45, 2020/01/01 2020.

[26] A. Fatahi-Vajari and A. Imam, "Axial vibration of single-walled carbon nanotubes using doublet mechanics," Indian Journal of Physics, journal article vol. 90, no. 4, pp. 447-455, 2016.

[27] A. Fatahi-Vajari and A. Imam, "Analysis of radial breathing mode of vibration of single-walled carbon nanotubes via doublet mechanics," ZAMM - Journal of Applied Mathematics and Mechanics / Zeitschrift

für Angewandte Mathematik und Mechanik, vol. 96, no. 9, pp. 1020-1032, 2016.

[28] A. Fatahi-Vajari and A. Imam, "Torsional vibration of single-walled carbon nanotubes using doublet mechanics," Zeitschrift für angewandte Mathematik und Physik, journal article vol. 67, no. 4, pp. 1-22, 2016.

[29] A. Fatahi-Vajari and Z. Azimzadeh, "Analysis of nonlinear axial vibration of single-walled carbon nanotubes using Homotopy perturbation method," Indian Journal of Physics, 2018/05/11 2018.

[30] U. Gul, M. Aydogdu, and G. Gaygusuzoglu, "Vibration and buckling analysis of nanotubes (nanofibers) embedded in an elastic medium using Doublet Mechanics," Journal of Engineering Mathematics, journal article May 29 2017.

[31] M. Haghgoo, R. Ansari, M.K. Hassanzadeh-Aghdam, 2022, Predicting effective electrical resistivity and conductivity of carbon nanotube/carbon black-filled polymer matrix hybrid nanocomposites, Journal of Physics and Chemistry of Solids, Volume 161, https://doi.org/10.1016/j.jpcs.2021.110444

[32] M. Noureddine, L. Mohamed, Y. Al-Douri, B. Djillali, B. Mokhtar, Effect of chiral angle and chiral index on the vibration of single-walled carbon nanotubes using nonlocal Euler-Bernoulli beam model, Computational Condensed Matter, 2022, volum 30, https://doi.org/10.1016/j.cocom.2022.e00655

[33] G. Dong, L. Pan, T. Huang, Y. Chen, N. Liao, T. Zhu, Q. Wang, S. Liang, J. Xu, Y. Wang, 2023, Stress intensity factor and fatigue crack propagation assessment of mode-I failure in alumina-calcium hexaluminate refractories, Open Ceramics, volume 15, https://doi.org/10.1016/j.oceram.2023.100422

[34] Ao Zhang, Wanlin Guo, 2024, Stress intensity factors and fatigue growth life of crescent-shaped cracks initiated from a spherical cavity, International Journal of Fatigue, volume 181, https://doi.org/10.1016/j.ijfatigue.2024.108156

[35] Y. Jiang, J. Sun, Q. Lin, J. Xiang, 2023, A two-stage method to detect damages in aluminum plates using curvature modal shape subtraction indicator and particle swarm optimization, Thin-Walled Structures, volume 185, https://doi.org/10.1016/j.tws.2023.110560

[36] J. Pacheco-Chérrez, D. Cárdenas, O. Probst, 2021, Experimental Detection and Measurement of Crack-Type Damage Features in Composite Thin-Wall Beams Using Modal Analysis, Sensors 2021, 21(23), 8102; https://doi.org/10.3390/s21238102

[37] M. R. Ebrahimian, Z. Azimzadeh, A. Fatahi-Vajari, M. Shariati, 2021, Nonlinear coupled torsional-radial vibration of single-walled carbon nanotubes using numerical methods, Journal of Computational Applied Mechanics 2021, 52(4), pp. 642-663; https: 10.22059/JCAMECH.2021.333435.661

[38] M. R. Ebrahimian, D. Shokri, B. Tabibian, M. R. Allahverdlou, M. S. Atlasbaf 2023, Analytical Response of Nonlinear Buckling of Composite Plates Reinforced with Graphene Nanosheets, Transactions on Machine Intelligence 2023, 6(2), pp. 76-88; https: 10.47176/TMI.2023.76

[39] P. M. Naghdi, The Theory of Shells and Plates. Springer-Verlag Berlin Heidelberg, 1972.

[40] N. Silvestre, "On the accuracy of shell models for torsional buckling of carbon nanotubes," European Journal of Mechanics - A/Solids, vol. 32, pp. 103-108, 3// 2012.